2

Compression of Surface Electromyographic Signals Using Two-Dimensional Techniques

Marcus V. C. Costa[1], João L. A. Carvalho[1], Pedro A. Berger[2], Adson F. da Rocha[1] and Francisco A. O. Nascimento[1]
[1]*Department of Electrical Engineering*
[2]*Department of Computer Science*
University of Brasília
Brazil

1. Introduction

Surface electromyographic (S-EMG) signals provide non-invasive assessment of muscle function and structure (Merletti & Parker, 2004). The transmission and/or storage of S-EMG signals may be an issue, since the data volume of such signals is potentially large, depending on factors such as sampling rate, quantization precision, number of channels, and experiment duration. Although several techniques have been proposed for the compression of biomedical signals such as the electrocardiogram (ECG) and the electroencephalogram (EEG) (Naït-Ali & Cavaro-Ménard, 2008), few techniques are available for the compression of S-EMG signals.

The use of image encoding standards may provide several benefits to the compression of S-EMG signals. Such standards are well-established and widely-used, and fast and reliable implementations of these algorithms are readily-available in several operational systems, software applications, and portable systems. These aspects could be positive in the implementation of S-EMG data banks, as well as in telemedicine applications.

This chapter discusses the use of two-dimensional data encoders for compression of S-EMG signals measured during isometric contractions. The S-EMG data is first arranged into a $N \times M$ matrix, composed of M signal segments of length N. Then, a preprocessing step is used to increase the two-dimensional correlation of this matrix. This is achieved by rearranging the columns of the matrix such that the correlation between adjacent columns is maximized. Finally, arithmetic encoding is used to compress the column-order list, and an off-the-shelf image compression algorithm is used for reducing the data size.

The proposed approach is evaluated on eighteen S-EMG recordings measured on the *biceps brachii* muscle of four healthy male volunteers during isometric exercise. We graphically show the increase in two-dimensional correlation provided by the proposed preprocessing stage, and quantitatively demonstrate the improvement in compression efficiency achieved when such stage is used. Using the proposed approach, we show that off-the-shelf image encoders — namely the JPEG2000 and the H.264/AVC-intra algorithms — may be used for efficient compression of S-EMG signals. Finally, we quantitatively compare the performance

of these two algorithms with the S-EMG encoders proposed by Norris et al. (2001) and Berger et al. (2006).

2. Electromyographic Signals

Electromyography assesses muscle function by studying electrical signals generated by the musculature. Electromyographic signals (EMG) are relevant to the comprehension of human musculature and for the diagnosis of several neuromuscular diseases (Basmajian & De Luca, 1985; Merletti & Parker, 2004). However, the storage and transmission of such signals in telemedicine applications are still challenging, as the amount of data to transmit and store increases with sampling rate, sampling precision, number of channels, number of individuals, and other factors. Signal compression techniques may be useful in reducing the data size of electromyographic signals.

2.1 Motor unit and action potentials

In order to understand the nature of the EMG signal, it is important to first understand muscle physiology and the way muscles produce bioelectrical signals. There are three types of muscles in the human body: cardiac muscle (specialized heart tissue, with peculiar characteristics); skeletal muscle (also known as voluntary muscle, because it is controlled consciously); and smooth muscle (involuntary muscle, controlled unconsciously). The latter covers the surface of internal organs and is responsible for functions such as compressing the esophagic channel to complete the deglutition, or controlling the blood flow to several tissues.

The object of study of electromyography is skeletal muscle, which is connected directly or indirectly (by tendons) to the bones. Skeletal muscles work in antagonic pairs: while one of the muscles contracts, the other, which is responsible for the opposite movement of the joint, relaxes, producing different types of movements.

Skeletal muscle is composed of multiple bundles of muscle fibers. Muscle fibers are long and cylindrical multinucleated cells. In normal human skeletal muscle, muscle fibers do not contract individually. Instead, they contract in small groups called motor units. A motor unit is composed by a motor neuron, neuromuscular junctions, and the muscle fibers innervated by this neuron. The motor unit is the smallest functional unit of striated muscle (Basmajian & De Luca, 1985).

The impulse that originates at the motor neuron, propagates along the spinal neuraxon, and reaches the muscle fiber, is called motor action potential, and is responsible for starting the muscle contraction process. When this impulse reaches the muscle fibers, it generates a muscle action potential. The wave created at the neuromuscular junction due to the excitation of the group of fibers that compose a motor unit is called motor unit action potential (MUAP). The MUAP propagates from the innervation area to the tendinous insertion, as well as in the opposite direction (Basmajian & De Luca, 1985).

2.2 Surface vs. intramuscular electromyography

Electromyography is based on extracellular assessment of the events described above. Intramuscular and surface electromyographic techniques are supplementary to each other, and both are relevant instruments for physiological investigation. Intramuscular

electromyography is an invasive technique which uses needles or microelectronic devices placed directly in contact with the muscle. This technique is more appropriate and widely accepted for clinical applications, although it causes pain and discomfort to the patient.
Surface electromyography, also known as non-invasive electromyography, uses metal electrodes (typically Ag/AgCl) placed over the skin. S-EMG has wide application in areas such as biofeedback, prosthesis control, ergonomics, occupational medicine, sports medicine, and movement analysis. S-EMG allows painless access to neuromuscular functions, thus providing additional versatility. The measured S-EMG signal is a record of the sum of several MUAPs. The MUAPs are activated asynchronously, thus the measured signal is stochastic and highly complex (Figure 1). The extraction of clinical relevant patterns from S-EMG signals is a difficult problem. Consequently, the knowledge about such signal is not as broad as in the field of electrocardiography, for example (Merletti & Parker, 2004).

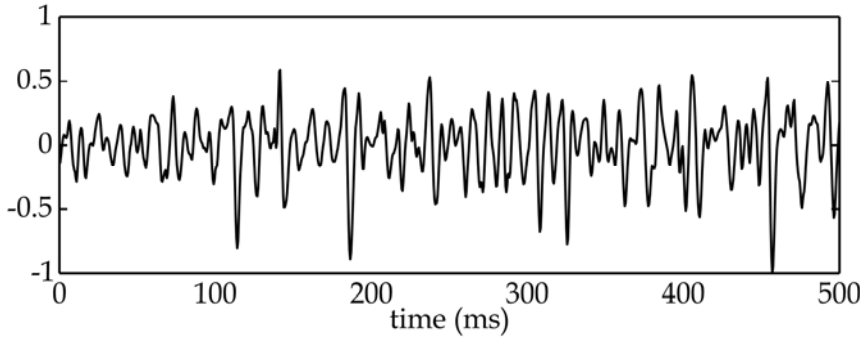

Fig. 1. S-EMG signal measured on the *biceps brachii* during an isometric contraction.

3. Signal Compression Techniques

Digitization of biomedical signals has been used for many different applications, such as ambulatory monitoring, phone line transmission, database storage, and several other uses in health and biomedical engineering. These applications have helped in diagnostics, patient care, and remote treatment. One example is the digital transmission of ECG signals, from the patient's home or ambulance to the hospital. This has been proven useful in cardiac diagnosis.
Biomedical signals need to be digitally stored or transmitted using a large number of samples per second, and with a large number of bits per sample, in order to ensure waveform fidelity, required for visual inspection. The use of signal compression techniques is fundamental for cost reduction and technical feasibility of storage and transmission of biomedical signals.
The purpose of any signal compression technique is the reduction of the amount of bits used to represent a signal. This must be accomplished while preserving the morphological characteristics of the waveform. In theory, signal compression is the process where the redundant information contained in the signal is detected and eliminated. Shannon (1948) defined redundancy as one minus "the ratio of the entropy of a source to the maximum value it could have while still restricted to the same symbols".

Signal compression has been widely studied in the past decades (Gersho & Gray, 1992; Jayant & Noll, 1984; Sayood, 2005; Salomon, 2006). Signal compression techniques are commonly classified into two categories: lossless and lossy compression. Lossless compression means that the decoded signal is identical to the original signal. In lossy compression, a controlled amount of distortion is allowed. Lossy signal compression techniques generally achieve higher compression rates than lossless techniques.

3.1 Lossless compression

Lossless signal compression techniques are less efficient with respect to compression rate than lossy compression. Lossless compression may be used in combination with lossy compression techniques, especially in cases where the maximum allowed distortion has been reached, and additional compression is needed. Among several lossless compression techniques, we highlight run-length encoding (Jayant & Noll, 1984), Huffman encoding (Huffman, 1952), arithmetic encoding (Witten et al., 1987), and differential encoding (Jayant & Noll, 1984).

3.1.1 Run-length encoding

Data files frequently present sequentially repeated characters, i.e., a character run. For example, text files use several spaces to separate sentences and paragraphs. Digital signals may contain the same value, or the same character representing that value, sequentially repeated many times in its data file. This indicates that the signal is not changing.

Figure 2 shows an example of run-length encoding (Jayant & Noll, 1984) of a data set that contains runs of zeros. Each time the encoder finds a zero in the entry data, two values are written in the output data. The first of these values is a zero indicating that run-length codification started. The second value is the amount of zeros in the sequence. If the run of zeros in the input data set is in average larger than two, then run-length encoding will achieve data compression.

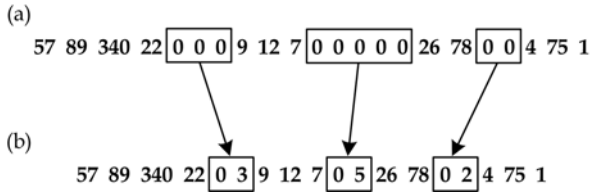

Fig. 2. Example of run-length encoding: (a) original signal; (b) encoded signal.

3.1.2 Huffman encoding

In Huffman encoding (Huffman, 1952), the data are represented as a set of variable-length binary words. The length depends on the frequency of occurrence of the symbols used for representing each signal value. Characters that are used often are represented with fewer bits, and seldom-used characters are represented with more bits.

Figure 3 shows an example of how a Huffman code is generated, given a symbol X, and its characteristic probability of occurrence, $p(X)$. The character codes are generated by combining the bits of a tree with ramifications, adding their probabilities, and then restarting the process until only one character remains. This process generates a tree with

ramifications linked to bits 0 and 1. The codes for each character are taken in the inverse path of these ramifications. Note that initial character arrangement is not relevant. In this example, we chose to encode the upper ramifications with bit 0 and the lower ones with bit 1. However, the opposite representation could also have been used. Any decision criteria may be used in ramifications with equal probabilities.
Huffman encoding has the disadvantage of assigning an integer number of bits to each symbol. This is a suboptimal strategy, because the optimal number of bits per symbol depends on the information content, and is generally a rational number.

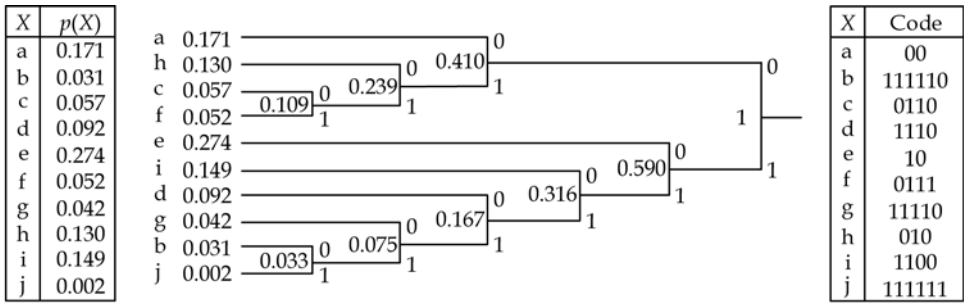

Fig. 3. Huffman code construction example.

3.1.3 Arithmetic encoding

Arithmetic encoding (Witten et al., 1987) is based on Huffman encoding concepts, but is more sophisticated, and achieves compression rates closer to the theoretical limits. Character sequences (symbols) are represented by individual codes, depending on their probability of occurrence, or a probability model.
At initialization, the [0,1) interval is divided into subintervals, with length proportional to its associated symbol probability. Every time a symbol appears in the message, its corresponding subinterval is divided into subintervals proportional to the symbol probabilities. When the end of the message is reached, the algorithm chooses a floating point value within the interval associated with the last encoded symbol. The binary representation of this value represents the message. This principle is illustrated in Figure 4, which shows the step-by-step encoding process for the message "BACADEA", with probability model: $p(A)=3/7$, $p(B)=1/7$, $p(C)=1/7$, $p(D)=1/7$ and $p(E)=1/7$.

3.1.4 Differential encoding

Differential pulse code modulation (DPCM) (Jayant & Noll, 1984) refers to signal compression techniques that represent the digital signal as the sequence of differences between successive samples. Figure 5 shows an example of how this is performed. The first sample in the encoded signal is equal to the first sample of the original signal. Subsequent encoded samples are equal to the difference between the current sample and the previous sample of the original signal. Using this technique, the encoded signal has a smaller amplitude dynamic range than the original signal. Therefore, fewer bits are needed to store or transmit the encoded signal. DPCM is used in combination with Huffman encoders in several biomedical signal compression algorithms.

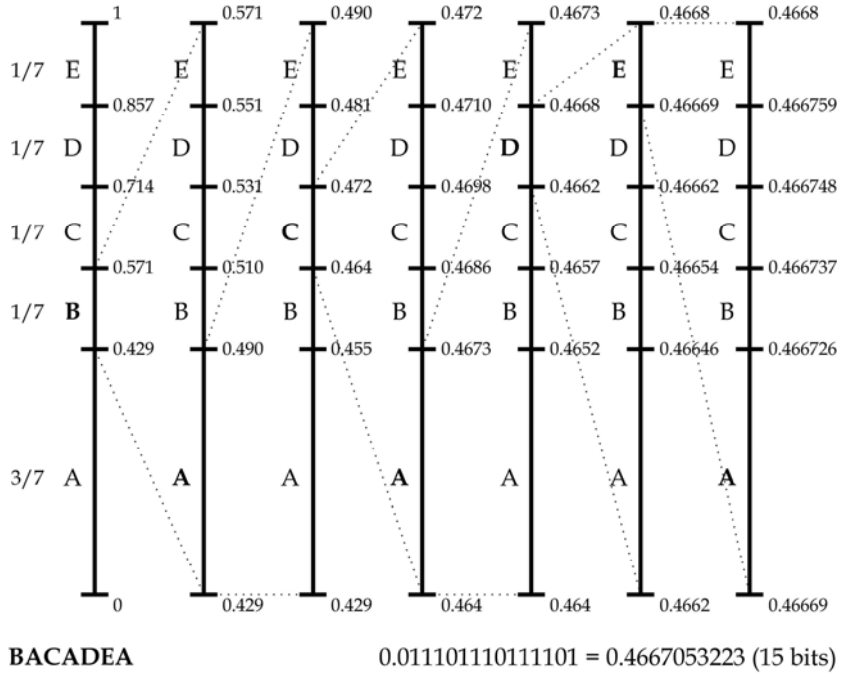

Fig. 4. Step-by-step arithmetic encoding process for the message "BACADEA", with probability model: $p(A)=3/7$, $p(B)=1/7$, $p(C)=1/7$, $p(D)=1/7$ and $p(E)=1/7$.

(a)
44 73 78 60 63 29 46 42 52 31 ...

(b)
44 29 5 -18 3 -34 17 -4 10 -21 ...

Fig. 5. Differential encoding example: (a) original signal; (b) encoded signal.

3.2 Lossy compression

There are two main categories of lossy compression techniques used with biomedical signals: direct methods and transform compression.

3.2.1 Direct methods

Direct methods encode signals in time domain. These algorithms depend on the morphology of the input signal. In most cases, these methods are complex, and provide lower compression efficiency than transform encoders (discussed in the next section).

Direct compression methods use sophisticated processes and "intelligent" signal decimation and interpolation. In other words, these methods extract K "significant" samples of the original length-N signal, $x(n)$, i.e.:

$$\left(n, x(n)\right),\ n = 0,...,N-1 \rightarrow \left(n_k, x(n_k)\right),\ k = 0,...,K-1\ , \tag{1}$$

where $K<N$. The process of selecting significant samples is based on the characteristics of the signal, and on a tolerance interval criterion for the reconstruction error.
The reconstruction of values between significant samples is performed by interpolation, using the generic expression (Sörnmo & Laguna, 2006):

$$\tilde{x}(n) = \begin{cases} x(n) & n = n_0,...,n_{K-1}; \\ f_{n_0,n_1}(n), & n = n_0+1,...,n_1-1; \\ \vdots & \vdots \\ f_{n_{K-2},n_{K-1}}(n), & n = n_{K-2}+1,...,n_{K-1}-1. \end{cases} \tag{2}$$

The interpolation function, $f_{n_{k-1},n_k}(n)$, is generally a first-order polynomial, and connects pairs of consecutive significant samples. Only K samples are stored, instead of N, resulting in a reduction of the amount of stored or transmitted data.

3.2.2 Transform encoding

Among the several methods for signal compression, techniques based on transforms achieve the best performance in terms of compression gain and waveform fidelity. For a data vector x, we can define an orthogonal transform as a linear operation given by a linear transformation T, such that:

$$y = Tx\ , \tag{3}$$

where y represents a vector of transformed coefficients, and T satisfies the orthogonality condition:

$$T^t = T^{-1}\ . \tag{4}$$

Transform compression is based on a simple premise: when the signal is processed by a transform, the signal energy (information) that was distributed along all time-domain samples can be efficiently represented with a small number of transform coefficients.
This is illustrated in Figure 6, where a two-dimensional signal is shown along with its corresponding coefficients in transform domain. In this example, we use the discrete cosine transform (DCT). The DCT is used in the most widely used standard for image compression, the Joint Picture Expert Group (JPEG) format.
Currently, the most widely used transform for encoding biomedical signals is the discrete wavelet transform (Daubechies, 1988; Mallat, 1989; Vetterli & Kovačević, 1995; Strang & Nguyen, 1996). In this transform, a signal containing N samples is filtered using a pair of filters that decompose the signal into low (L) and a high (H) frequency bands. Each band is undersampled by a factor of two; that is, each band contains $N/2$ samples. With the appropriate filter design, this process is reversible. This procedure can be extended to two-dimensional signals, such as images. In Figure 7, we show an example of wavelet decomposition for a gray-scale image with 256×256 pixels. Similarly to what was observed

using the DCT, many of the coefficients in the high-frequency subbands have amplitudes close to zero (dark pixels), and it is possible to compress the image by discarding them.

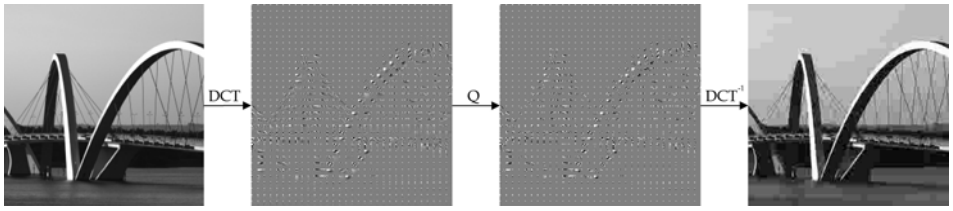

Fig. 6. Example of DCT-based image compression, applied in blocks of 8×8 pixels (Q denotes quantization).

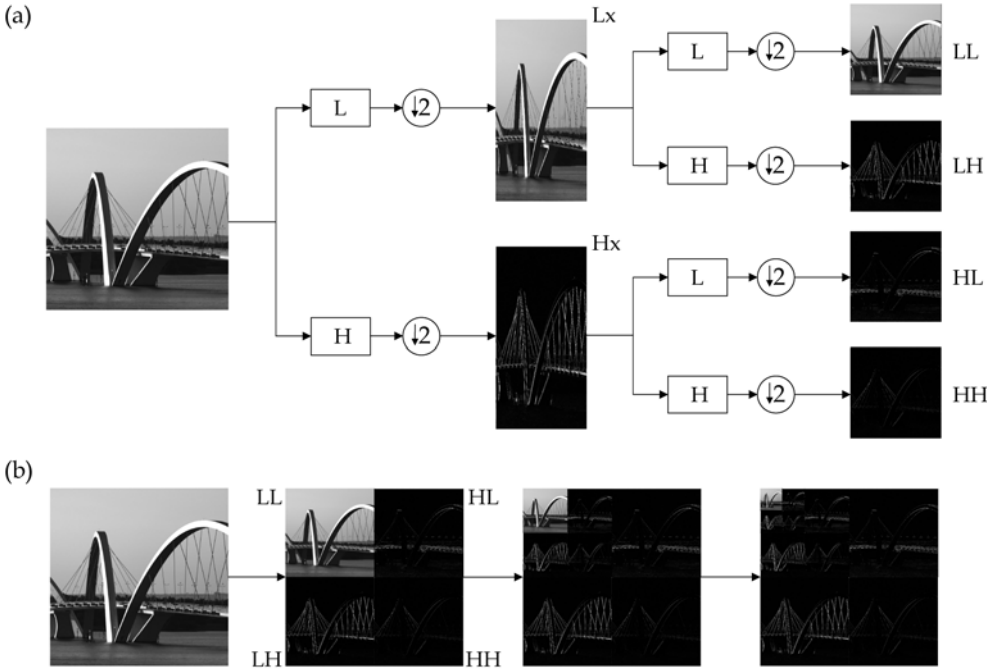

Fig. 7. Example of a 2D wavelet decomposition: (a) step-by-step one-level decomposition; (b) three-level decomposition.

Wavelet transform compression is evolving with respect to the way in which the coefficients are encoded. When a coefficient in a low-frequency subband is nonzero, there is a high probability that, at positions that correspond to high frequencies, the coefficients are also nonzero. Thus, the nonzero coefficients can be represented in a tree, starting at a low frequency root. Figure 8 illustrates this concept. Each coefficient in the LL band of level 1 has a corresponding coefficient in the other bands. The position of each coefficient in level 1 is mapped into four daughter-positions in each subband of level 2. An efficient way of encoding the coefficients that are nonzero is to encode each tree of coefficients, beginning

with the root decomposition level. The coefficients at the lower levels are encoded, and followed by their children coefficients in the higher level, until a null coefficient is found. The next coefficients of the tree have large probability of also being null, and are replaced by a code that identifies a tree of zeros (zerotree code). This method is called embedded zerotree wavelet (EZW) (Shapiro, 1993). A similar approach, commonly used in wavelet coefficient encoding, is the set partitioning in hierarchical trees (SPIHT) method (Said & Pearlman, 1996).

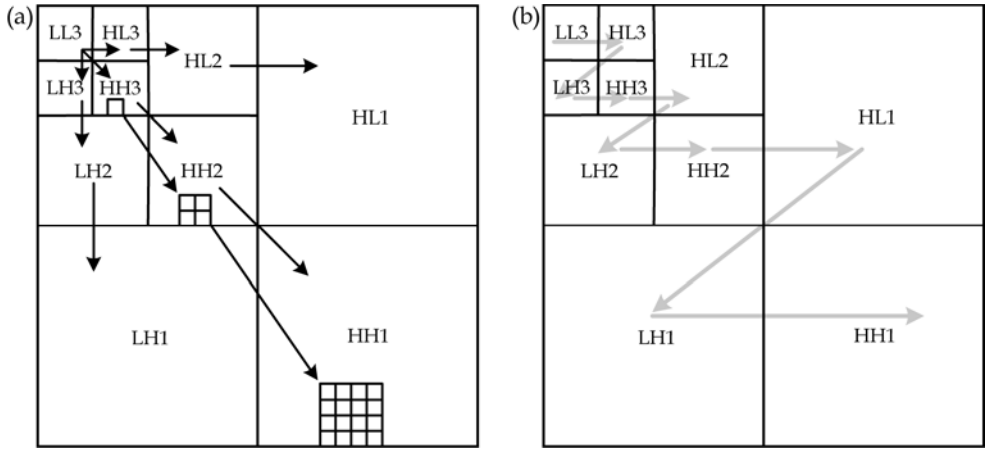

Fig. 8. EZW method: (a) zerotree data structure; (b) coefficients scanning order.

Modern image and video encoding algorithms are based on transform-domain approaches. For example, the JPEG2000 algorithm (Taubman, 2000; Taubman & Marcellin, 2002; Acharya & Tsai, 2004) is a state-of-the-art image encoding standard which uses embedded block coding with optimal truncation (EBCOT) (Taubman, 2000) on the subband samples of the discrete wavelet transform of the image. The H.264/AVC encoder (Richardson, 2003; Wiegand et al., 2003; Sullivan et al., 2004) is the latest standard for video compression, and uses a low-complexity integer discrete cosine transform.

4. Compression of S-EMG Signals

Different approaches have been proposed for compression of electromyographic signals. Norris & Lovely (1995) investigated the compression of electromyographic signals using adaptive differential pulse code modulation (ADPCM). Guerrero & Mailhes (1997) compared different compression methods based on linear prediction and orthogonal transforms. They showed that methods based on the wavelet transform outperform other compression methods. The use of the EZW algorithm has also been proposed for compression of electromyographic signals (Wellig et al., 1998; Norris et al., 2001). More recently, Berger et al. (2006) proposed an algorithm for compression of electromyographic signals using the wavelet transform and a scheme for dynamic bit allocation of the coefficients using a Kohonen layer. In a recent work, Brechet et al. (2007) adopted the

discrete wavelet packet transform decomposition with optimization of the mother wavelet and of the basis of wavelet packets, followed by an EZW-like encoder. The use of speech encoding methods has also been reported in the literature (Guerrero & Mailhes, 1997; Carotti et al., 2006). Carotti et al. (2006) proposed a scheme for compression of simulated and real EMG signals with algebraic code excited linear prediction (ACELP) and the results were evaluated with several spectral and statistics measurements. Filho et al. (2008a) adopted a multiscale multidimensional parser algorithm. Paiva et al. (2008) proposed adaptive EMG compression using optimized wavelet filters. Two of these methods are discussed in detail below.

Norris et al. (2001) proposed a S-EMG compression algorithm based on one-dimensional EZW, and compared its performance with that of standard wavelet compression methods, using both isometric and isotonic signals. They showed that the EZW based approach performed consistently better than standard wavelet approaches.

The algorithm proposed by Berger et al. (2006) is a transform domain encoder that uses a dynamic bit allocation scheme that adapts to the local signal statistics in wavelet domain. The S-EMG signal is segmented in blocks of 2048 samples, and the wavelet transform is applied to each block. The transform coefficients go through a normalization stage, which leads to a large number of null coefficients. The bit allocation scheme, which is implemented using a Kohonen neural network, assigns a specific amount of bits to quantize the coefficients in each frequency sub-band interval (Figure 9). The Kohonen layer represents a dictionary of 64 possible bit allocation vectors. Thus, six bits are used to identify the bit allocation scheme used in each transform block. The transform coefficients in each block are quantized using the associated bit allocation vector, and the quantized coefficients, Kohonen dictionary index, and normalization factors are then Huffman encoded and stored/transmitted. In the decoder, the quantized coefficients are recovered using the overhead information (dictionary index and normalization factor), and the decoded signal segments are obtained using the inverse wavelet transform.

5. Two-Dimensional S-EMG Compression

One-dimensional signals may be compressed using image encoding algorithms, simply by rearranging the signal samples into a two-dimensional matrix, which may be processed as an image. This approach has been previously demonstrated in the field of electrocardiography. For example, the JPEG2000 image encoding algorithm has been efficiently applied to ECG signal compression (Bilgin et al., 2003; Chou et al., 2006). Similarly, the H.264/AVC-intra encoder has also been used (Filho et al., 2008b). Two-dimensional encoding methods based on the discrete wavelet transform, followed by SPIHT coefficient encoding, have also been proposed (Lu et al., 2000; Pooyan et al., 2004; Miaou & Chao, 2005; Moazami-Goudarzi et al., 2005; Rezazadeh et al., 2005; Tai et al., 2005; Sharifahmadian et al., 2006; Sahraeian & Fatemizadeh, 2007). This section investigates the use of image encoding algorithms for compression of S-EMG signals.

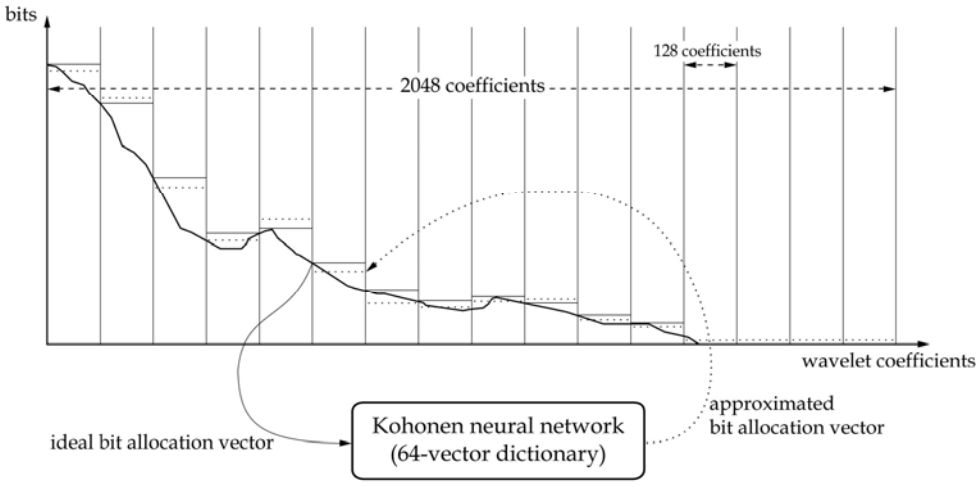

Fig. 9. Illustration of the quantization algorithm used in the encoder proposed by Berger et al. (2006). Each block of 2048 wavelet coefficients is divided into 16 sub-bands with 128 spectral lines. The ideal bit allocation vector is constructed using the number of bits necessary to quantize the largest coefficient in each sub-band. This is used as input of a Kohonen neural network, which outputs the approximated bit allocation vector.

5.1 Two-dimensional S-EMG modeling

S-EMG signals of isometric contractions are usually modeled as stochastic processes. The typical autocorrelation function associated with S-EMG signals indicates a stationary or, at least, locally stationary process.

In two-dimensional compression of S-EMG signals, the one-dimensional vector is segmented in M windows of length N, and arranged into a $N \times M$ matrix (Figure 10). This leads us to a two-dimensional real random field, $x_s[n,m]$, where: $n = 0, 1, \ldots, N-1$; $m = 0, 1, \ldots, M-1$; $s \in \Omega$; and $\Omega = \{1,2,\ldots\}$ is the sample space (Figure 11). The 2D matrix associated with each possible realization corresponds to a different two-dimensionally rearranged S-EMG signal.

The two-dimensionally arranged data can be seen as a homogeneous random field, because it is assumed that one-dimensional S-EMG signal is a stationary stochastic process. A random field is called homogeneous if its expected value of $x[n,m]$, μ_x, is independent of position $\vec{v}$, i.e., $\mu_x(\vec{v}) = \mu_x$. For rearranged S-EMG data, $\mu_x = 0$.

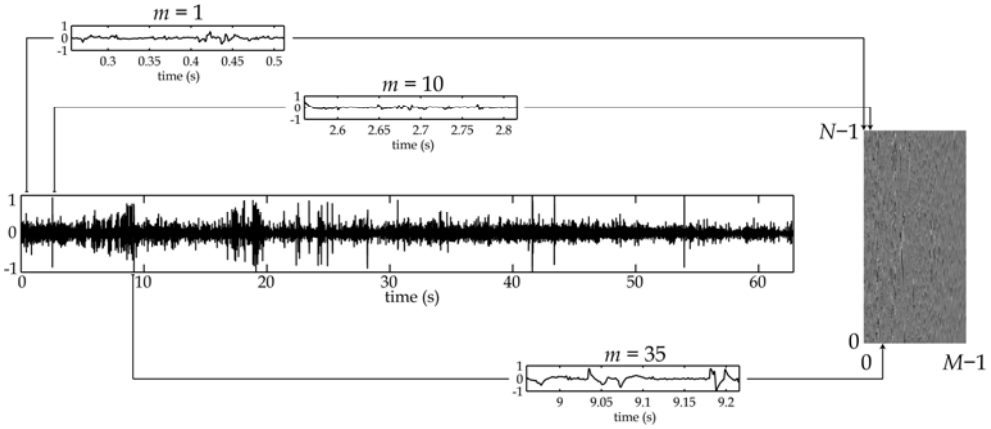

Fig. 10. One-dimensional S-EMG signal rearranged into a two-dimensional matrix.

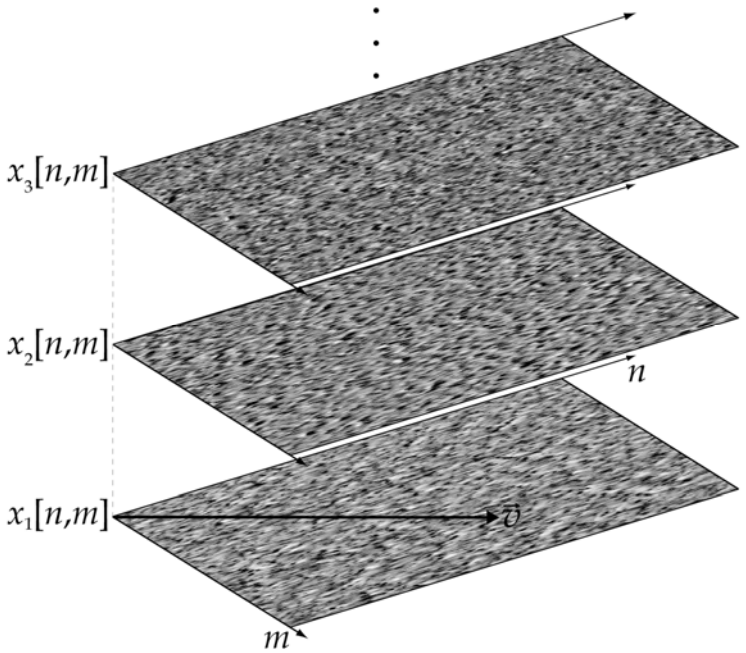

Fig. 11. Two-dimensional real random field, x_s [n,m], showing multiple realizations of two-dimensionally arranged S-EMG signals.

Homogeneous random fields present translation invariant autocorrelation functions, i.e.:

$$R_x(\vec{v}_1,\vec{v}_2) = R_x\{x(\vec{v}_1)x(\vec{v}_2)\} \equiv R_x(\vec{v}_1-\vec{v}_2) \equiv R_x(\vec{v}_2-\vec{v}_1)\ . \tag{5}$$

If we denote the position vectors $\vec{v}_1$ and $\vec{v}_2$ by their respective pair of discrete coordinates *m*, *n* and *j, i*, respectively, then the autocorrelation function can be expressed as

$$R_x(n,m,i,j) = R_x[n-i,m-j] = R_x[i-n,j-m] \ . \tag{6}$$

If we use the discrete variables *k* and *r* to denote the coordinate differences *n*−*i* and *m*−*j*, respectively, the above equation can be rewritten as

$$R_x(n,m,i,j) = R_x[k,r] = R_x[-k,-r] \ . \tag{7}$$

In general, the autocorrelation function of a random field is a function of four variables. However, the autocorrelation function of a homogeneous random field (e.g., S-EMG data) is a function of only two variables, *k* and *r*:

$$R_x[k,r] = E\{x[n,m]x[n+k,m+r]\} = \sum_{n=0}^{N-1}\sum_{m=0}^{M-1} x[n,m]x[n+k,m+r] \ . \tag{8}$$

The autocovariance function, $C_x[k,r]$, is defined as

$$C_x[k,r] = E\{x[n,m]x[n+k,m+r] - \mu^2\} = \sum_{n=0}^{N-1}\sum_{m=0}^{M-1}\left(x[n,m]x[n+k,m+r] - \mu^2\right) . \tag{9}$$

Under the assumption that a class of rearranged S-EMG data forms a homogeneous random field, the autocorrelation function, $R_x[k,r]$, may be assumed to be of the form

$$R_x[k,r] = \left(R_x[0,0] - \mu^2\right)e^{-\alpha|k|-\beta|r|} + \mu^2 \ , \tag{10}$$

where α and β are positive constants (Rosenfeld & Kak, 1982), and where, by definition,

$$R_x[0,0] = E\left\{\left(x[n,m]\right)^2\right\} = \sum_{n=0}^{N-1}\sum_{m=0}^{M-1} x[n,m]^2 \ , \text{ and} \tag{11}$$

$$\mu = E\{x[n,m]\} = \frac{1}{NM}\sum_{n=0}^{N-1}\sum_{m=0}^{M-1} x[n,m] = 0 \ . \tag{12}$$

For rearranged S-EMG data, $\mu = 0$, and the autocorrelation function is reduced to:

$$R_x[k,r] = R_x[0,0]e^{-\alpha|k|-\beta|r|} = C_x[k,r] \ . \tag{13}$$

Constants α and β can be distinct, due to the nature of rearranged S-EMG data. This means that the autocorrelation function can be used to model two-dimensional data with different degrees of correlation in the horizontal and vertical directions, by specifying the values of α and β. In our method, one direction corresponds to linear time data sampling, with strong

correlation, and the other corresponds to window step, and leads to weak correlation. The correlation along the window step direction may be increased using column reordering based on inter-column correlation, as discussed in the next section.
Figure 12a presents the theoretical autocorrelation function, calculated using equation (13), with a=0.215 and β=0.95. Figure 12b presents the autocorrelation function associated with the S-EMG shown in Figure 10, after column reordering. These results demonstrate that two-dimensionally arranged S-EMG data presents two-directional correlation and two-dimensional redundancy. Therefore, this type of data may be compressed using image compression techniques. In the next section, we present a technique for maximizing two-dimensional S-EMG correlation and thus improving compression efficiency.

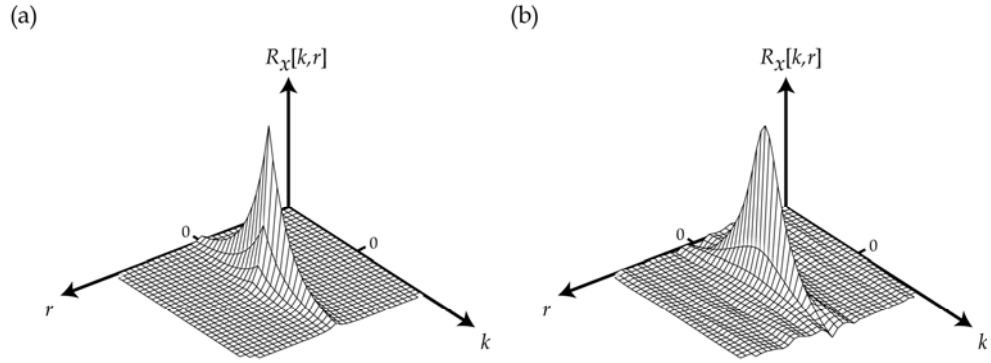

Fig. 12. Autocorrelation functions: (a) computed from the theoretical model, using a=0.215 and β=0.95; (b) computed from the data shown in Figure 10.

5.2 Correlation sorting

Adjacent samples of S-EMG signals are typically moderately temporally-correlated. When the S-EMG signal is arranged into a 2D matrix, this feature is preserved along the vertical dimension (columns). However, such correlation is generally lost along the horizontal dimension (rows). In order to increase 2D-compression efficiency, we attempt to increase the correlation between adjacent columns, by rearranging the columns based on their cross-correlation coefficients.
The matrix of column cross-correlation coefficients (R) is computed from the covariance matrix C, as follows:

$$R(u,w) = \frac{C(u,w)}{\sqrt{C(u,u)\cdot C(w,w)}} \ . \tag{14}$$

Then, the pair of columns that present the highest cross-correlation coefficient is placed as the first two columns of a new matrix. The column that presents the highest cross-correlation with the second column of the new matrix is placed as the third column of the new matrix, and so forth. A list of column positions in annotated. This procedure is similar

to that used by Filho et al. (2008b) for reordering segments of ECG signals, but the similarity metric used in that study was the mean squared error. Figure 13 illustrates the result of applying the proposed column-correlation sorting scheme to a S-EMG signal arranged in 2D representation.

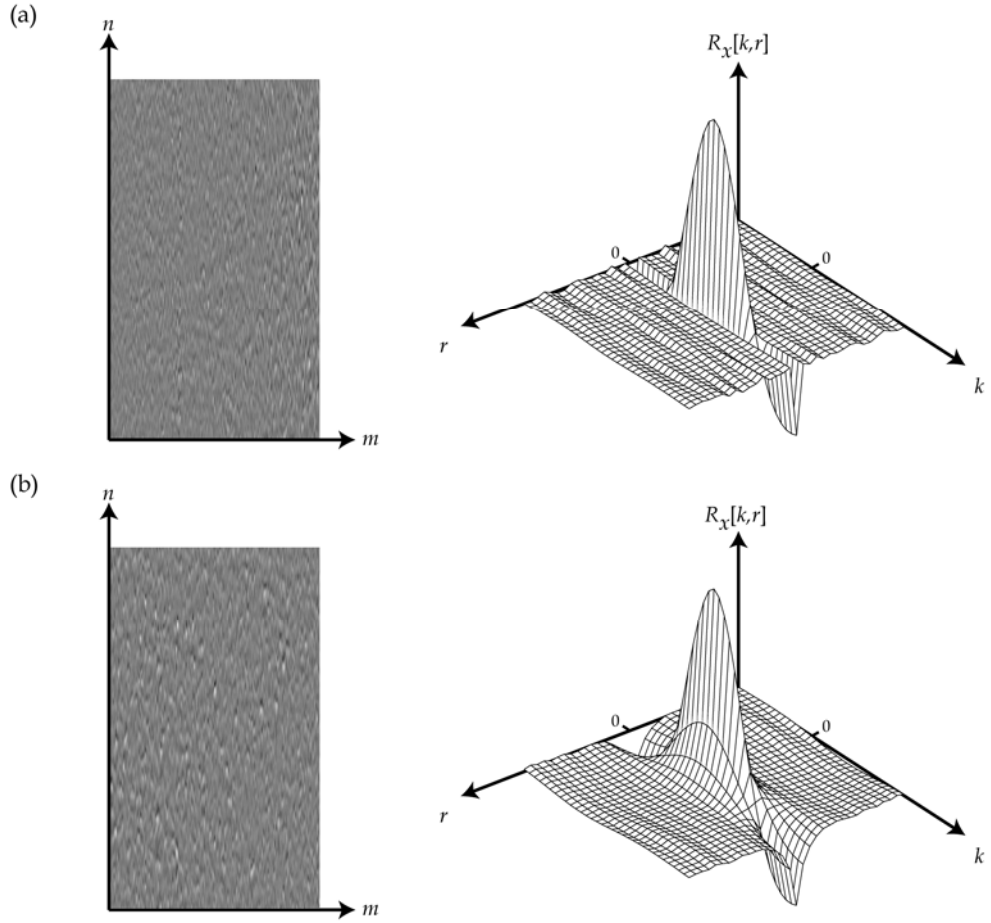

Fig. 13. Two-dimensionally arranged S-EMG signal (left) and associated autocorrelation function (right): (a) without correlation sorting; (b) with correlation sorting.

5.3 Image compression techniques applied to 2D-arranged S-EMG

Figure 14 shows a block diagram of the proposed encoding scheme. The method consists in segmenting each S-EMG signal into 512-sample windows, and then arranging these segments as different columns of a two-dimensional matrix, which can then be compressed using 2D algorithms. In this work, we investigated the use of two off-the-shelf image encoders: the JPEG2000 algorithm, and the H.264/AVC encoder.

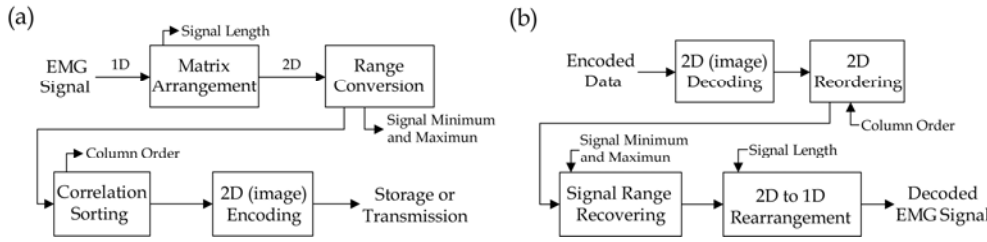

Fig. 14. Block diagram of the proposed compression algorithm: (a) encoder; (b) decoder.

The number of columns in the 2D matrix is defined by the number of 512-sample segments. The last (incomplete) segment is zero-padded. The matrix is scaled to the 8-bit range (0 to 255). The columns are rearranged, based on their cross-correlation coefficients. The matrix is encoded using one of the above-mentioned image encoders. The list of original column positions is arithmetically encoded. Scaling parameters (maximum and minimum amplitudes) and number of samples are also stored (uncompressed).
The encoded matrix is recovered using the appropriate image decoder, and the S-EMG signal is reconstructed by scaling the signal back to its original dynamic range and then rearranging the matrix columns back into a one-dimensional vector.

5.4 Experimental methods

A commercial electromyograph (Delsys, Bagnoli-2, Boston, USA) was used for signal acquisition. This equipment uses active electrodes with a pre-amplification of 10 V/V and a pass-band of 20–450 Hz. The signals were amplified with a total gain of 1000 V/V, and sampled at 2 kHz using a 12-bit data acquisition system (National Instruments, PCI 6024E, Austin, TX, USA). LabView (National Instruments, Austin, TX, USA) was used for signal acquisition, and Matlab 6.5 (The MathWorks, Inc., Natick, MA, USA) was used for signal processing.
Isometric contraction EMG signals were obtained from 4 male healthy volunteers with 28.3 ± 9.5 years of age, 1.75 ± 0.04 m height, and 70.5 ± 6.6 kg weight. Signals were measured on the *biceps brachii* muscle. In the beginning of the protocol, the maximum voluntary contraction (MVC) was determined for each subject. The signals were collected during 60% MVC contraction, with an angle of 90° between the arm and the forearm, and with the subject standing. The protocol was repeated 5 times for each volunteer, with a 48-hour interval between experiments. One of the volunteers was absent during two of the sessions. Therefore, a total of 18 EMG signals were acquired.
The JPEG2000 algorithm was evaluated with compression rates ranging from 0.03125 to 8 bits per pixel. The H.264/AVC encoder was used in intraframe (still image) mode, with DCT quantization parameter values ranging from 51 to 1.
The compression quality was evaluated by comparing the reconstructed signal with the original signal. The performance of the compression algorithm was measured by two quantitative criteria: the compression factor (CF) and the square root of the percentage root mean difference (PRD). These two criteria are widely used for evaluating the compression of S-EMG signals. The compression factor is defined as

$$\mathrm{CF}(\%) = \frac{Os - Cs}{Os} \cdot 100 \,, \tag{15}$$

where *Os* is the number of bits required for storing the original data, and *Cs* is the number of bits required for storing the compressed data (including overhead information). The PRD is defined as

$$\mathrm{PRD}(\%) = \sqrt{\frac{\sum_{n=0}^{N-1} (x[n] - \tilde{x}[n])^2}{\sum_{n=0}^{N-1} x^2[n]}} \cdot 100 \,, \tag{16}$$

where x is the original signal, $\tilde{x}$ is the reconstructed signal, and N is the number of samples in the signal.

5.5 Results

Figure 15 shows the mean PRD (as a function of CF) measured on the set of 18 isometric S-EMG signals, using the JPEG2000 and H.264/AVC-intra compression algorithms, after correlation-based column-reordering. The quality decreases (PRD increases) when the compression factor is increased. With the JPEG2000 algorithm, compression factors higher than 88% causes significant deterioration of the decoded signal. With the H.264/AVC-intra algorithm, the results show significant degradation for compression factors higher than 85%. Figure 16 illustrates the compression quality for a S-EMG signal measured during isometric muscular activity. The central 2500 samples of the original, reconstructed, and error signals are shown. In this example, correlation sorting (*c.s.*) was used, with 75% compression factor. The PRD was measured to be 2.81% and 4.65% for the JPEG2000 and H.264/AVC-intra approaches, respectively. The noise pattern observed for both approaches seems visually uncorrelated with the signal.

Table 1 shows mean PRD values measured using different compression algorithms, for isometric contraction signals. The JPEG2000-based method provided slightly better reconstruction quality (lower PRD) than the EZW-based algorithm by Norris et al. (2001) for compression factors values ≤85%. However, this difference was not statistically significant. Compared with the method by Berger et al. (2006), JPEG2000 showed moderately inferior overall performance. This is especially true for 90% compression, in which its performance is comparable to that achieved by Berger et al. The H.264/AVC-based method showed low overall performance. The signal acquisition protocols used by Norris et al. (2001) and Berger et al. (2006) were similar to the one used in this work: 12-bit resolution, 2 kHz sampling rate, S-EMG isometric contractions measured on the *biceps brachii* muscle. However, some details of the acquisition protocols were not discussed in the work by Norris et al., (e.g., the distance between electrodes). The signals used in that work may present characteristics that are relevantly different from the those of the signals used in this work.

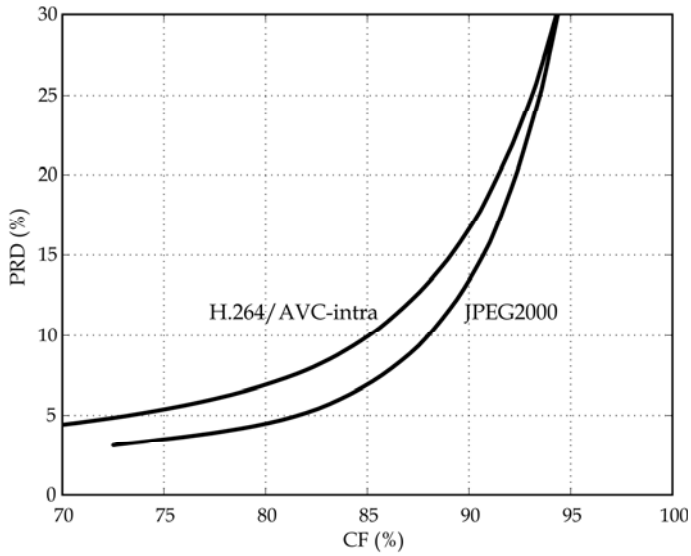

Fig. 15. Compression performance comparison (CF vs. PRD) between the JPEG2000 and H.264/AVC-intra image encoders, using the correlation sorting preprocessing step.

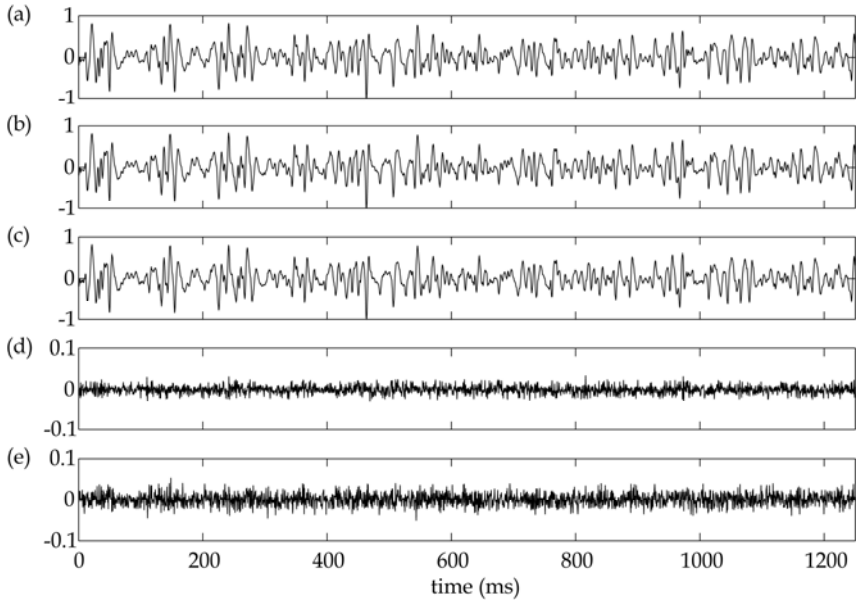

Fig. 16. Representative results for a 1250-ms segment of a S-EMG signal. (CF=75%): (a) uncompressed; (b) *c.s.* + JPEG2000; (c) *c.s.* + H.264/AVC-intra; (d) JPEG2000 reconstruction error; (e) H.264/AVC-intra reconstruction error. Reconstruction errors are magnified by 10-fold.

Compression Factor	75%	80%	85%	90%
Norris et al.	3.8	5	7.8	13
Berger et al.	2.5	3.3	6.5	13
JPEG2000	3.58	4.60	7.05	13.63
c.s. + JPEG2000	3.50	4.48	6.92	13.44
H.264/AVC-intra	5.51	7.03	10.01	16.68
c.s. + H.264/AVC-intra	5.37	6.90	9.93	16.62

Table 1. Mean PRD (in %) for isometric contraction signals.

The improvement in compression performance achieved using the proposed preprocessing stage (correlation-based column reordering) was not significant (Table 1). Column reordering increases inter-column correlation and improves compression efficiency. However the addition of overhead information increases the overall data size, resulting in similar PRD values. Better results may be achieved in the context of isotonic contractions, in which data redundancy is more significantly increased by the proposed approach.

6. Conclusions

This chapter presented a method for compression of surface electromyographic signals using off-the-shelf image compression algorithms. Two widely used image encoders were evaluated: JPEG2000 and H.264/AVC-intra. We showed that two-dimensionally arranged electromyographic signals may be modeled as random fields with well-determined autocorrelation function properties. A preprocessing step was proposed for increasing inter-column correlation and improving 2D compression efficiency.

The proposed scheme was evaluated on surface electromyographic signals measured during isometric contractions. We showed that commonly available algorithms can be effectively used for compression of electromyographic signals, with a performance that is comparable or better than that of other S-EMG compression algorithms proposed in the literature. We also showed that correlation sorting preprocessing may potentially improve the performance of the proposed method.

The JPEG2000 and H.264/AVC-intra image encoding standards are well-established and widely-used, and fast and reliable implementations of these algorithms are readily-available in several operational systems, software applications, and portable systems. These are important aspects to be considered when selecting a compression scheme for specific biomedical applications, and represent promising features of the proposed approach.

7. References

Acharya, T. & Tsai, P. S. (2004). *JPEG2000 Standard for Image Compression: Concepts, Algorithms and VLSI Architectures*. John Wiley & Sons, ISBN 9780471484226, Hoboken, NJ, USA.

Basmajian, J. V. & De Luca, C. J. (1985). *Muscles Alive: Their Functions Revealed by Electromyography*. Williams & Wilkins, ISBN 9780683004144, Baltimore, USA.

Berger, P. A.; Nascimento, F. A. O.; do Carmo, J. C. & da Rocha, A. F. (2006). Compression of EMG Signals with Wavelet Transform and Artificial Neural Networks, *Physiological Measurement*, Vol. 27, No. 6, pp. 457–465, ISSN 1361-6597.

Bilgin, A.; Marcellin, M. W. & Altbach, M. I. (2003). Compression of Electrocardiogram Signals using JPEG2000. *IEEE Transactions on Consumer Electronics*. Vol. 49, No. 4, pp. 833–840, ISSN 0098-3063.

Brechet, L.; Lucas, M.-F.; Doncarli, C. & Farina, D. (2007). Compression of biomedical signals with mother wavelet optimization and best-basis wavelet packet selection. *IEEE Transactions on Biomedical Engineering*, Vol. 54, No. 12, pp. 2186–2192, ISSN 0018-9294.

Carotti, E. S. G.; De Martin, J. C.; Merletti, R. & Farina, D. (2006). Compression of surface EMG signals with algebraic code excited linear prediction. *Proceedings of IEEE International Conference on Acoustics, Speech and Signal Processing*, pp. 1148–1151, ISBN 142440469X, Tolouse, France, May 2006.

Chou, H-H.; Chen, Y-J.; Shiau, Y-C. & Kuo, T-S. (2006). An effective and efficient compression algorithm for ECG signals with irregular periods. *IEEE Transactions on Biomedical Engineering*, Vol. 53, No. 6, pp. 1198–1205, ISSN 0018-9294.

Daubechies, I. (1988). Orthogonal bases of compactly supported wavelets. *Communications on Pure and Applied Mathematics.* Vol. 41, No. 7, pp. 909–996, ISSN 0010-3640.

Filho, E. B. L.; da Silva, E. A. B. & de Carvalho, M. B. (2008a). On EMG signal compression with recurrent patterns. *IEEE Transactions on Biomedical Engineering*, Vol. 55, No. 7, pp. 1920–1923, ISSN 0018-9294.

Filho, E. B. L.; Rodrigues, N. M. M.; da Silva, E. A. B.; de Faria, S. M. M.; da Silva, V. M. M. & de Carvalho, M. B. (2008b). ECG signal compression based on DC equalization and complexity sorting. *IEEE Transactions on Biomedical Engineering*, Vol. 55, No. 7, pp. 1923–1926, ISSN 0018-9294.

Gersho, A. & Gray, R. (1992). *Vector quantization and signal compression*. Kluwer Academic Publishers, ISBN 0792391810, Norwell, MA, USA.

Guerrero, A. P. & Mailhes, C. (1997). On the choice of an electromyogram data compression method. *Proceedings of the 19th Annual International Conference of the IEEE Engineering in Medicine and Biology Society*, pp. 1558–1561, ISBN 0780342623, Chicago, IL, USA, Oct. 30-Nov. 2 1997.

Huffman, D. A. (1952). A method for the construction of minimum-redundancy codes. *Proceedings of the Institute of Radio Engineers*, Vol. 40, No. 9, pp. 1098–1101.

Jayant, N. S. & Noll, P. (1984). *Digital coding of waveforms – principles and application to speech and video*. Prentice Hall, Inc., ISBN 9780132119139, Englewood Cliffs, NJ, USA.

Lu, Z.; Kim, Y. D. & Pearlman, A. W. (2000). Wavelet compression of ECG signals by the set partitioning in hierarchical trees algorithm. *IEEE Transactions on Biomedical Engineering*. Vol. 47, No. 7, pp. 849–856, ISSN 0018-9294.

Mallat, S. G. (1989). A theory for multiresolution signal decomposition: the wavelet representation. *IEEE Transactions on Pattern Analysis and Machine Intelligence.* Vol. 11, No. 7, pp. 674–693, ISSN 0162-8828.

Merletti, R. & Parker, P. (2004). *Electromyography: Engineering and Noninvasive Applications*, John Wiley & Sons – IEEE Press, ISBN 9780471675808, Hoboken, NJ, USA.

Miaou, S. & Chao, S. (2005). Wavelet-based lossy-to-lossless ECG compresion in a unified vector quantization framework. *IEEE Transactions on Biomedical Engineering.* Vol. 52, No. 3, pp. 539–543, ISSN 0018-9294.

Moazami-Goudarzi, M.; Moradi, M. H. & Abbasabadi, S. (2005). High performance method for electrocardiogram compression using two dimensional multiwavelet transform. *IEEE 7th Workshop on Multimedia Signal Processing*, pp. 1–5, ISBN 0780392884, Shanghai, Oct. 30-Nov. 2 2005.

Naït-Ali, A. & Cavaro-Ménard, C. (2008). *Compression of Biomedical Images and Signals,* ISTE - John Wiley & Sons, ISBN 9781848210288, London, UK - Hoboken, NJ, USA.

Norris, J. A.; Englehart, K. & Lovely, D. (2001). Steady-state and dynamic myoelectric signal compression using embedded zero-tree wavelets, *Proceedings of 23rd Annual International Conference of the IEEE Engineering in Medicine Biology Society*, pp. 1879–1882, ISBN 0780372115, Istanbul, Turkey, Oct. 2001.

Norris, J. F. & Lovely, D. F. (1995). Real-time compression of myoelectric data utilizing adaptive differential pulse code modulation. *Medical and Biological Engineering and Computing*, Vol. 33, No. 5, pp. 629–635, ISSN 0140-0118.

Paiva, J. P. L. M.; Kelencz, C. A.; Paiva, H. M.; Galvão, R. K. H. & Magini, M. (2008). Adaptive wavelet EMG compression based on local optimization of filter banks, *Physiological Measurement*, Vol. 29, No. 7, pp. 843–856, ISSN 1361-6597.

Pooyan, M.; Moazami-Goudarzi, M. & Saboori, I. (2004). Wavelet compression of ECG signals using SPIHT algorithm. *IEEE International Journal of Signal Processing*, Vol. 1, No. 4, pp. 219–225, ISSN 2070-397X.

Rezazadeh, I. M.; Moradi, M. H. & Nasrabadi, A. M. (2005). Implementing of SPIHT and sub-band energy compression (SEC) method on two-dimensional ECG compression: a novel approach. *27th Annual International Conference of the Engineering in Medicine and Biology Society,* pp. 3763–3766. ISBN 0780387414, Shanghai, 17-18 Jan. 2006.

Richardson I. E. G. (2003). *H.264 and MPEG-4 Video Compression: Video Coding for Next-generation Multimedia*. Wiley, ISBN 9780470848371, UK.

Rosenfeld, A. & Kak, A. C. (1982). *Digital picture Processing (Volume 1): 2nd Ed.* Academic Press. Inc, ISBN 0125973012, San Diego, CA, USA.

Sahraeian, S. M. E. & Fatemizadeh, E. (2007). Wavelet-based 2-D ECG data compression method using SPIHT and VQ coding. *The International Conference on "Computer as a Tool", EUROCON, 2007*, pp. 133–137. ISBN 9781424408139, Warsaw, 9-12 Sept. 2007.

Said, A. & Pearlman, W. A. (1996). A new, fast, and efficient image codec based on set partitioning in hierarchical trees. *IEEE Transactions on Circuits and Systems for Video Technology*, Vol. 6, No. 3, pp. 243–250. ISSN 1051-8215.

Salomon, D. (2006). *Data Compression: The Complete Reference, 4th ed.*, Springer, ISBN 9781846286025, London, UK.

Sayood, K. (2005). *Introduction to Data Compression, 3rd ed.*, Morgan Kaufmann Publishers, ISBN 9780126208627, San Francisco, CA, USA.

Shannon, C. E. (1948). A mathematical theory of communication. *Bell System Technical Journal,* Vol. 27, July and October, pp. 379-423 and 623-656.

Shapiro, J. M. (1993). Embedded image coding using zerotrees of wavelet coefficients. *IEEE Transactions on Signal Processing,* , Vol. 41, No. 12, pp. 3445–3462, ISSN 1053-587X.

Sharifahmadian, E. (2006). Wavelet compression of multichannel ECG data by enhanced set partitioning in hierarchical trees algorithm. *28th Annual International Conference of the IEEE Engineering in Medicine and Biology Society*, pp. 5238–5243, New York City, USA, July 30-Aug. 3 2006.

Sörnmo, L. & Laguna, P. (2006). Electrocardiogram (ECG) signal processing. In: *Wiley Encyclopedia of Biomedical Engineering (Vol. 2)*, Metin Akay (Ed.), pp. 1298–1313, John Wiley & Sons, ISBN 9780471249672.

Strang, G. & Nguyen, T. (1996). *Wavelets and Filter Banks*. Wellesley-Cambridge Press, ISBN 0961408871, Wellesley, MA, USA.

Sullivan, G.; Topiwala, P. & Luthra, A. (2004). The H.264/AVC advanced video coding standard: Overview and introduction to the fidelity range extensions. *Proceedings of SPIE Conference on Applications of Digital Image Processing XXVII, Special Session on Advances in the New Emerging Standard: H.264/AVC*, Vol. 5558 (2), pp. 454–474. ISBN 0819454966, Denver, CO, USA, 2-6 August 2004.

Tai, S-C.; Sun C-C. & Yan, W-C. (2005). A 2-D ECG compression method based on wavelet transform and modified SPIHT. *IEEE Transactions on Biomedical Engineering,* Vol. 52, No. 6, pp. 999–1008, ISSN 0018-9294.

Taubman, D. S. & Marcellin, M. W. (2002), *JPEG2000: Image Compression Fundamentals, Standards and Practice*, Springer, ISBN 079237519X, Boston, USA.

Taubman, D. S. (2000). High performance scalable image compression with EBCOT. *IEEE Transactions on Image Processing*, Vol. 9, No. 7, pp. 1158–1170, ISSN 1057-7149.

Vetterli, M. & Kovačević, J. (1995) *Wavelets and Subband Coding*, Prentice-Hall, ISBN 0130970808, Englewood Cliffs, NJ, USA.

Wellig, P.; Zhenlan, C.; Semling, M. & Moschytz G. S. (1998). Electromyogram data compression using single-tree and modified zero-tree wavelet encoding. *Proceedings of the 20th Annual International Conference of the IEEE Engineering in Medicine and Biology Societ,* ISBN 0780351649, pp. 1303–1306. Hong Kong, China, Oct. 29-Nov. 1 1998.

Wiegand, T.; Sullivan, G. J.; Bjontegaard, G. & Luthra, A. (2003). Overview of the H.264/AVC video coding standard. *IEEE Transactions on Circuits and Systems for Video Technology*, Vol. 13, No. 7, pp. 560–576, ISSN 1051-8215.

Witten, I.; Neal, R. & Cleary, J. (1987). Arithmetic coding for data compression. *Communications of the ACM*, Vol. 30, No. 6, pp. 520–540, ISSN 0001-0782.